INTERNATIONAL JOURNAL OF CLIMATOLOGY
Int. J. Climatol. **20**: 1131–1148 (2000)

COMPARATIVE SURFACE ENERGY BUDGETS IN WESTERN AND CENTRAL SUBARCTIC REGIONS OF CANADA

R.M. PETRONE[a,*], W.R. ROUSE[a] and P. MARSH[b]

[a] *School of Geography and Geology, McMaster University, 1280 Main St. West, Hamilton, Ontario, Canada L8S 4K1*
[b] *National Water Research Institute, 11 Innovation Blvd., Saskatoon, Saskatchewan, Canada S7N 3H5*

ABSTRACT

The surface energy balance was measured over two summer seasons (1996 and 1997) at three Canadian subarctic sites. These were a wetland site in the central subarctic and a wetland and dryland site in the western subarctic. These sites have similar temperature regimes but the central subarctic site receives twice as much rainfall as each of the western sites. The sites display substantial differences in their surface characteristics. A comparison between the three study sites allows definition of the impact of surface controls on the surface energy budget, for the two subarctic locations. By comparing the evaporation rates between these three sites the surface control mechanisms at the local scale (i.e. microtopography, vegetation cover and organic layer thickness) can be examined relative to the larger scale geographical factors. The two wetland sites demonstrated similar evaporation behaviour but the dryland evaporates substantially less. This similarity in wetland evaporation in spite of major differences in rainfall and standing water demonstrates the importance of the surface organic layer in transporting and storing water for evaporation. The magnitude of convective and conductive heat fluxes is strongly correlated with temperature in both regions. Warm temperatures enhance the latent and ground heat fluxes while suppressing the sensible heat flux at all sites. Cold temperatures have the opposite effect. Copyright © 2000 Royal Meteorological Society.

KEY WORDS: subarctic; surface energy balance; region; evaporation; technique(s); climate variable(s)

1. INTRODUCTION

Regional energy balances exert a major control on climatic and hydrologic regimes in northern environments. With contemporary concern on the potential effects of climate warming, knowledge of interactions of changes in air temperature with the energy balance is important. Subarctic latitudes are known to be very sensitive to climate change. General circulation models (GCMs) indicate that these latitudes could experience an increase in temperature of 4–5°C under a $2 \times CO_2$ scenario by the year 2100 (Intergovernmental Panel on Climate Change, 1992). Such warmer temperatures would bring about an earlier snowmelt, enhanced absorbed radiant energy, an increase in evapotranspiration, and a change in the ground heat flux (Rouse, 1990).

Seasonally, evapotranspiration accounts for approximately 50% of precipitation across the mainland area of subarctic and arctic North America and somewhat less among the Arctic Islands (Maxwell, 1997). This amount can be even greater during the summer in areas of low relief, such as the numerous lakes, bogs and wetlands of the Arctic mainland (Woo *et al.*, 1992). These extensive wetlands possess an abundance of peat which controls the availability of moisture for evaporation (Maxwell, 1997).

The surface energy budget is complicated by the inherent heterogeneity of these environments. Heterogeneity is responsible for spatial changes in the partitioning of the surface available energy (net radiation minus the ground heat flux) between the fluxes of sensible and latent heat, due to differences in the surface thermal, radiative, hydraulic and evapotranspirative properties (Guo and Schuepp, 1994).

Extraterrestrial and atmospheric controls such as those exerted by the solar radiation cycle and cloud cover affect the surface energy budget by altering the surface radiation balance. At the land–atmosphere

* Correspondence to: School of Geography and Geology, McMaster University, 1280 Main St. West, Hamilton, Ontario, Canada L8S 4K1.

interface, differences in topography, soil type, vegetation type, and ground moisture and thermal condition (eg. ice-rich permafrost) further complicate the partitioning of the surface energy budget, to varying extents and at various scales. Spatial variations cause advective effects that influence evapotranspiration rates. These advective effects operate at different scales. Local variations in surface characteristics can lead to advective effects from upwind surfaces. On a meso-scale, geographical influences such as onshore and offshore winds and orographic effects exert strong thermal and humidity influences. At synoptic scales, air mass movement and characteristics advect different atmospheric conditions, thereby interacting with the surface energy budget.

The objective of this paper is to examine the effects of differences in regional climate, vegetation, topography and substrate on the surface energy budget and evaporation regime. To meet this objective, these features were monitored over 2 years at western and central Canadian subarctic sites. The dominant land–atmosphere controls on the surface energy balance and evaporation regime are described here and contrasted between the two regions. The sensitivity of the surface energy balance to temperature forcing, which is a function of synoptic activity, is also discussed. To illustrate the most important of these influences western and central Canadian high subarctic sites are used to examine the effects of differences in regional climate, vegetation, topography and substrate on the surface energy budget and evaporation regime. The sensitivity of the surface energy balance to temperature forcing is analysed. In a companion paper (Petrone and Rouse, 2000) synoptic influences on the surface energy balance are detailed.

2. SITE AND CLIMATIC CHARACTERISTICS

2.1. Central wetland (Cw) site

The central subarctic (Cw) research site is located 26 km east of Churchill, Manitoba (58°45′N, 93°57′W) (Region C) in a high subarctic wetland tundra region near the shores of Hudson Bay (National Wetlands Working Group (NWWG), 1987) (Figure 1). The site is underlain by continuous permafrost and is located just northeast of Arctic treeline. Both the continental location and Hudson Bay influence the climate creating the high subarctic conditions of long, cold winters, short cool summers, and relatively low annual precipitation. Churchill has an average annual temperature of -7.2°C, and an average annual precipitation of 402 mm of which 181 mm falls as snow (Boudreau and Rouse, 1995).

The site is commonly described as a sedge wetland or fen (NWWG, 1987; Wessel, 1992; Rouse, 1998) and comprises hummocky terrain in flat, poorly-drained wetland tundra. Peat hummocks, that create the local relief, range in height from 0.10 to 0.45 m (Figure 2). The soil consists of an average 0.25 m of fibrous peat, overlying a very thin carbonate cobble layer, atop a mineral soil composed of thick glaciomarine silty clays. The bulk density increases from ~ 0.5 g cm^{-3} near the surface to ~ 1.8 g cm^{-3} at a depth of 0.4 m as the soil becomes more developed (Figure 3). The porosity and volumetric moisture content decrease with depth, through the peat and clay layers in the soil column. The depth of peat is fairly uniform in both hummocks and hollows (Figure 2).

In both 1996 and 1997, the active layer, as defined by soil temperatures greater than 0°C, increased from a depth of approximately 0.3 m near the beginning of the study period in early June, to depths below of 0.95 m by late August (Figure 4). By mid-August, temperatures at the top of the profile began to cool while temperatures at greater depths maintained their temperature.

The greatest diversity in type and density of vegetation occurs on the hummocks (Table I). The dominant vascular plants are sedges (*Carex aquatilis*, *C. limosa*, *C. saxitalis*, and *C. gynocrates*). Minor representatives are dwarf birch (*Betula glandulosa*), dwarf willow (*Salix* spp.), Labrador tea (*Ledum decumbens*, *L. groenlandicum*), purple saxifrage (*Saxifraga oppostifolia*), and various berry species. The sedges range in height from 0.05 to 0.45 m, and have a mean stem diameter of 0.01 m. The most abundant lichens are from the *Cetraria* and *Cladina* genera. In the hollows, only a few sedges (*C. limosa*) are found. The hollows are dominated by the moss *Scorpidium turgescens*, which wets and dries as the water table moves above and below the surface and with the rainfall–evaporation cycle.

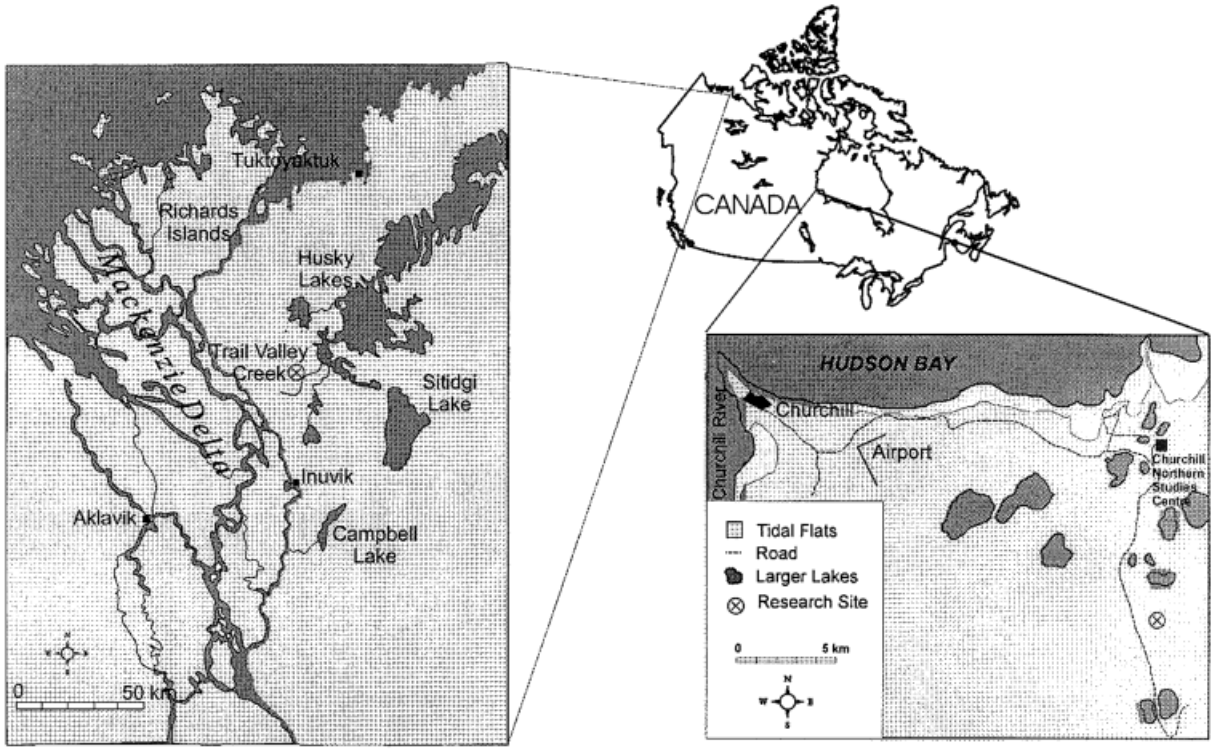

Figure 1. Location of the two study regions. Study sites are marked by ⊗

Rouse (1998) reports that the equilibrium position of the water table (i.e. water ponded after surface runoff) is on average, 0.08 m above the average bottom depths of the hollows. The growing conditions at this site are significantly influenced by the combination of microtopography and water table movement. Since hollows account for $\sim 50\%$ of the areal coverage of the fen, that same percentage of the fen is also saturated and anaerobic for about one-half of the growing season in an average year (Rouse, 1998).

2.2. Western wetland (Ww) site

The western subarctic wetland (Ww) site is located in the Trail Valley Creek (TVC) basin (68°45′N, 133°32′W), 56 km northeast of Inuvik, NWT (Region W) (Figure 1). This lies within the high subarctic region (Ecoregions Working Group, 1989) and is located on the Mackenzie River Delta, approximately 150 km from the coast of the Beaufort Sea and northeast of the Arctic treeline. Like Churchill, Inuvik experiences long, cold winters and short, cool summers, but experiences much less annual precipitation (Figure 5(b)). The climate is influenced both by its proximity to the Beaufort Sea to the north, and the Richardson Mountains to the west. TVC is situated in an abandoned glacial meltwater channel carved into a plateau, located at the northern fringe of the forest–tundra transition zone, within the zone of continuous permafrost (Quinton, 1997).

The Ww site is characterized as a low-lying, wetland. However, due to the site's slope down to TVC it is better drained than the Cw fen. The soil at Ww consists of 0.3 m of peat overlying a silty–clay layer (Figure 3). The top 0.10–0.15 m is composed of partially decomposed vegetation material and root systems. From 0.15 to 0.30 m the peat is more decomposed with slightly higher bulk densities and lower porosities. The bulk densities increase from 0.1 g cm^{-3} at the surface to 0.3 g cm^{-3} at a depth of 0.30 m.

During the 1996 and 1997 seasons, the active layer increased from a depth of 0.20 m at the beginning of the study period in mid-May, to 0.49 m by early September (Figure 4). The bottom portion of the

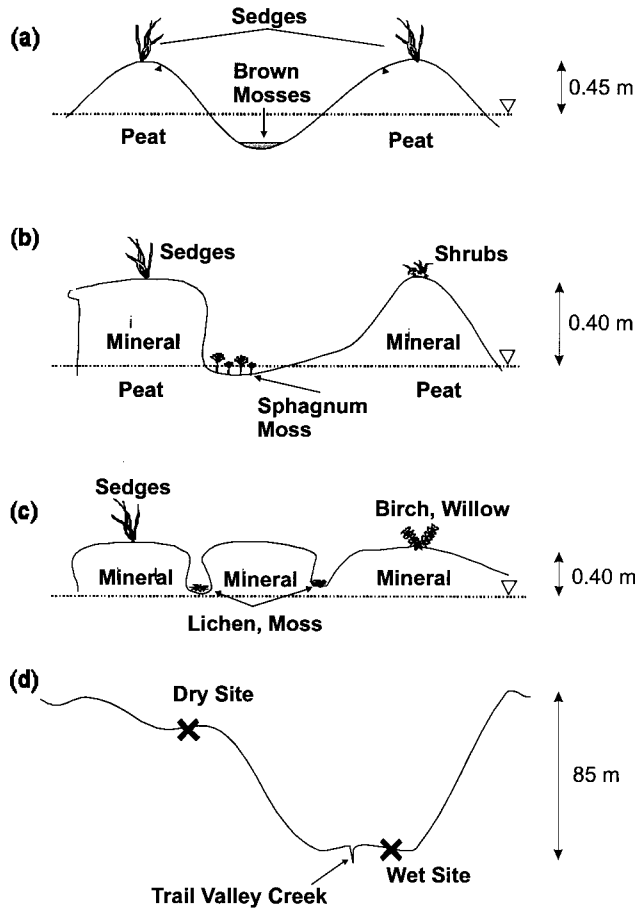

Figure 2. Schematic of microtopography at sites (a) Cw, (b) Ww and (c) Wd. (d) Indicates the relative topographic locations of Ww and Wd

profile did not warm any further after mid-August, and the top 0.35 m had cooled significantly by the end of that month.

Ww, like Cw, also has numerous hummocks and hollows, or interhummock areas, with local differences in relief of 0.20–0.40 m (Figure 2). In contrast to Cw, the hummock and interhummock areas at Ww have different soil composition. The hummocks are primarily mineral soils, whereas the interhummock areas are primarily peat (Figure 2). Hummocks may be bare, support a thin lichen layer, or have a sedge tussock cover with *Eriophorum* spp. and *Carex* spp. dominating (Figure 2). Many of the same lichens and vascular plants found at Cw are also found at Ww (Table I). However, the sedges and graminoids, which tend to dominate, are different species. Rather than *C. aquatilis* and *C. limosa*, the dominant sedge at Ww is *C. mackenzii*, and to a lesser extent, *C. aurea*. These sedges grow in tussocks, reach heights of approximately 0.10 m, and have a mean diameter of ~ 0.006 m. Other vascular plants found at the site, as at Cw, are *Ledum groenlandicum*, *B. glandulosa*, *S. arctophila*, and various berry species. Birch (*B. glandulosa*) at this site accounts for 20% of the total surface cover, and reaches maximum heights of ~ 0.45 m. The lichen *Cladina stellaris*, common at Cw, is scarce at this site. In contrast, *Alectoria nigricans* is quite abundant, but is absent at Cw. Ww hosts a thick covering of sphagnum moss (0.20–0.25 m) which is not seen in Cw.

The difference in dominant sedges and the extensive sphagnum cover at Ww may reflect the different moisture regimes. While both sites are wet, the hollows at Cw often maintain standing water and are thus frequently anaerobic. This dictates the species that can successfully grow. In contrast, Ww never exhibits ponded water and is aerobic, hence favouring the thick sphagnum mat.

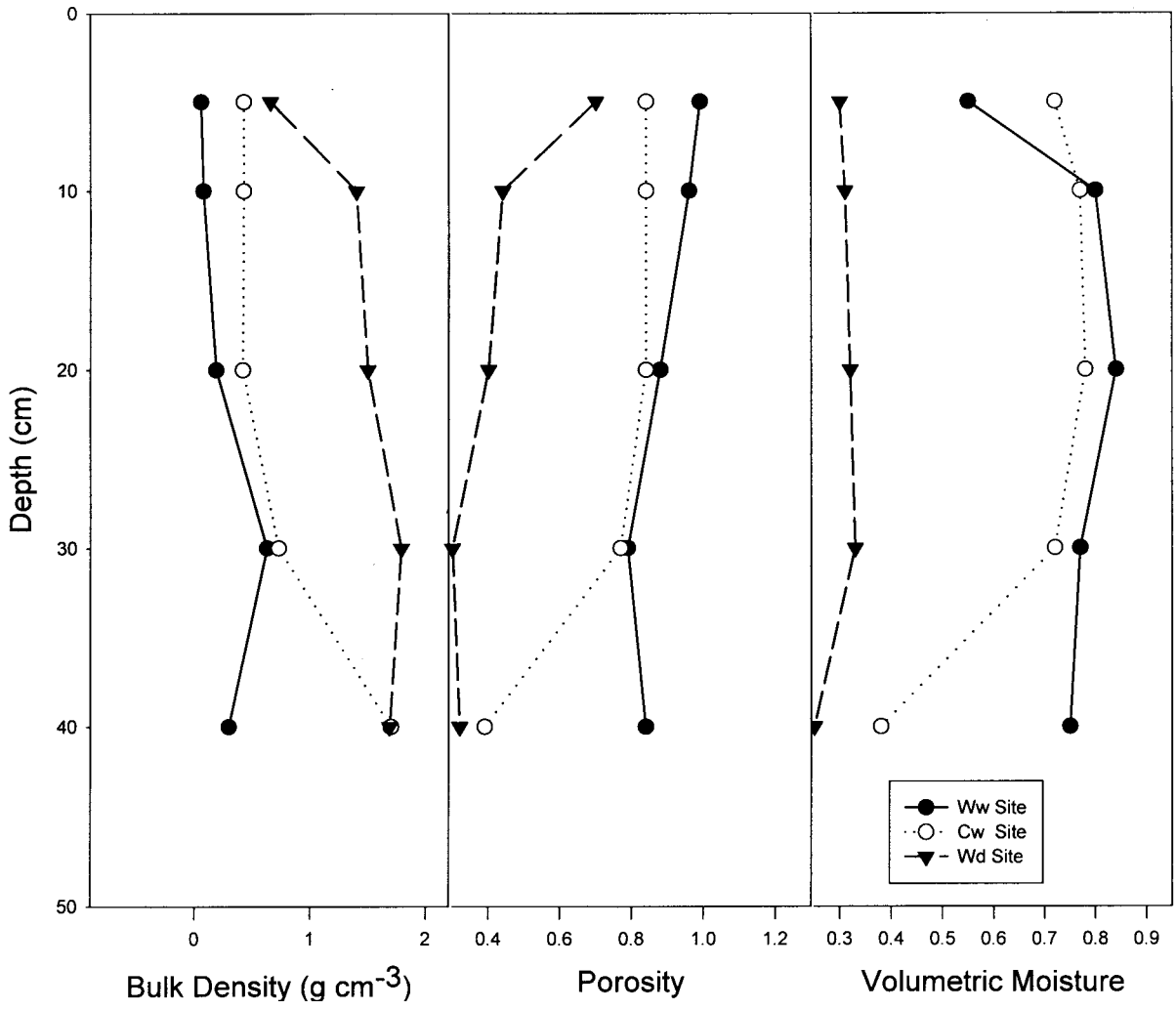

Figure 3. Depth profiles of the soil properties of the three sites

2.3. Western dry (Wd) site

The dry site, Wd (Figure 1) is located on a tundra plateau in the basin (Region W) at an elevation of approximately 85 m above sea level and approximately 1 km from the Ww site (Figure 2). Quinton (1997) has described the area as a rolling morainic terrain of early Wisconsin origin with a gentle hillslope gradient.

The soils are primarily mineral (Figure 3). Compared with the other sites, bulk densities are large and porosities and volumetric moisture contents are small. As at Ww, the interhummock areas are composed of organic soils, but, the organic layer is much thinner (Figure 2).

The active layer decreased from 0.30 m early in the season to depths greater than 0.80 m by early September, in both 1996 and 1997. Of all the sites, it is clear that the dry site experienced the most thawing with the largest temperature change over the course of a season (Figure 4).

The dominant microtopography is defined by mineral earth hummocks, which range in diameter from 0.40 to 1.00 m, with heights between 0.10 and 0.40 m. The hollows are narrower than at Ww appearing more as fissures (Quinton, 1997).

The dominant vegetation consists of lichens, mosses, and various berries and low deciduous shrubs (*Alnus*, *Betula*, *Salix*) (Marsh and Pomeroy, 1996) (Table I). The interhummock areas accommodate

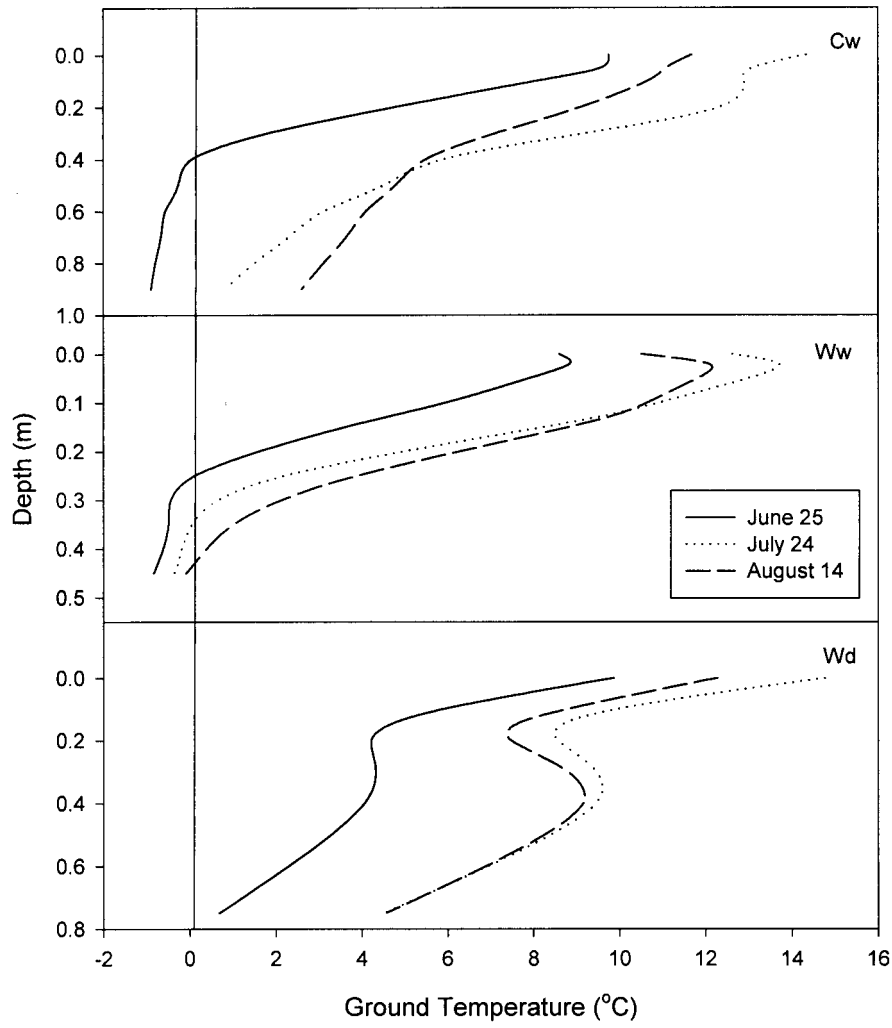

Figure 4. Ground temperature profiles for the three sites, early in the growing season, midsummer and late summer

sedges (*C. mackenziei* and *C. aurea*), dwarf willow and some dwarf birch. The deciduous shrubs at this site tend to be more clustered and dense than at Ww, accounting for approximately 25% of the surface cover, and ranging in height from 0.5 to 3.0 m.

2.4. Climatic comparisons

Meteorological records from the Churchill (Region C) and Inuvik (Region W) weather stations indicate only small differences in temperature but substantial differences in precipitation for the 40-year simultaneous record (1957–1997). Inuvik is cooler than Churchill (Figure 5), the direct result of its higher latitude and the strong cooling effects of the nearby Beaufort Sea. The relatively cool temperatures for Churchill are the result of the dominant northwesterly flow creating a strong continental influence during the fall and winter seasons, and the strong cooling influence of Hudson Bay during the spring and summer seasons. The linear trend of the mean annual temperature (over the last 40 years) indicates an increase in temperature of approximately 0.5°C and 0.3°C for Churchill and Inuvik, respectively (Figure 5(a)). Monthly mean maximum temperatures for both locations are observed in July and monthly mean minimum temperatures in January (Figure 5(b)). Inuvik's maximum summer temperature is greater than

Table I. Summary of the species of plants at the two study regions

	Region C	Region W
Sedges and Graminoids	*Carex aquatilis* *Carex limosa* *Carex rariflora* *Scirpus caespitosus*	*Carex mackenziei* *Carex aurea*
Mosses	*Scorpidium turgescens*	*Sphagnum* spp.
Lichen	*Cladina stellaris* *Cladina mitts* *Cladina rangiferina* *Cetraria nivalis* *Peltigera apthosa*	*Alectoria nigricans* *Cladina mitts* *Cladina rangiferina* *Ceuaria nivalis* *Peltigera apthosa* *Cladonia amauracraea*
Vascular plants	*Empetrum nigrum* *Vaccinium vitis-idaea* *Ledum decumbens* *Rubus chamemorus*	*Empetrum nigrum* *Vaccinium vitis-idaea* *Ledum groenlandicum* *Rubus chamaemorus*
Trees	*Betula glandulosa* *Salix arctophila*	*Betula glandulosa* *Salix arctophila*

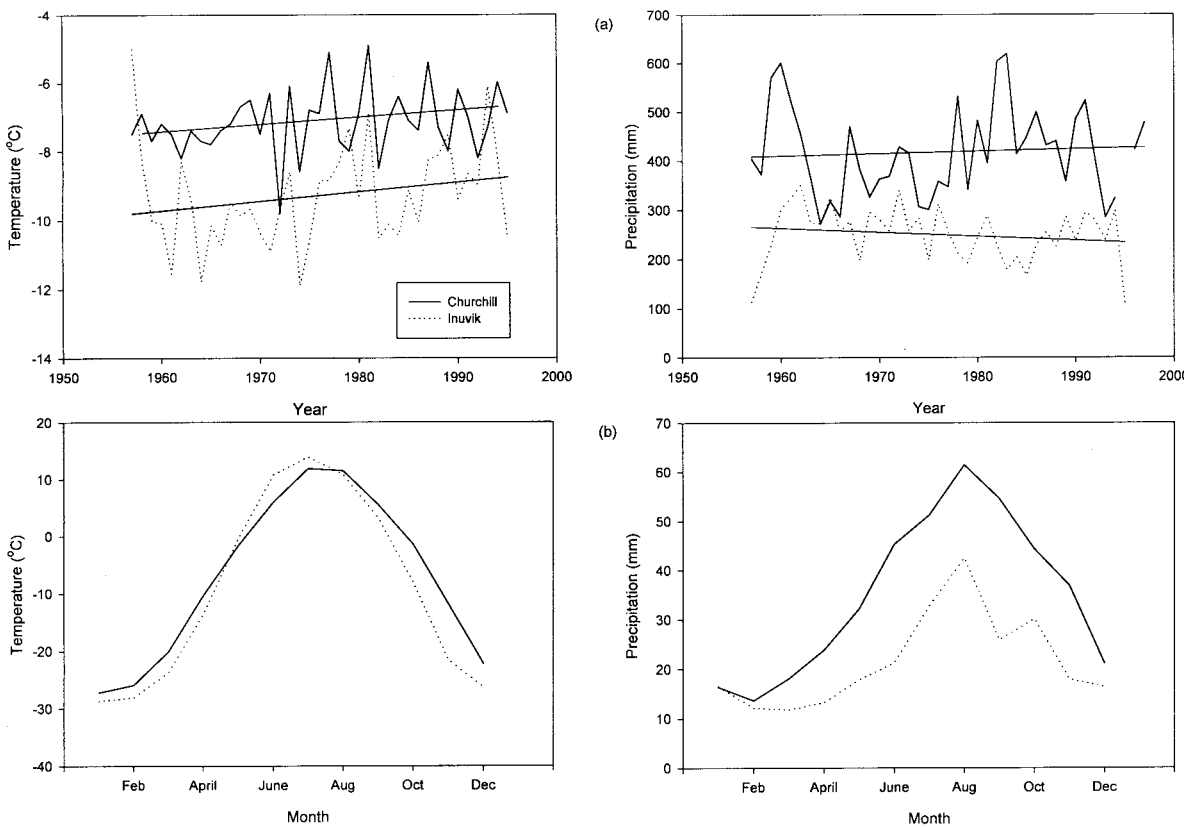

Figure 5. Annual mean temperatures and precipitation and monthly mean temperatures and precipitation at (a) Churchill and (b) Inuvik for the period 1957–1997

that for Churchill, due to the long hours of daylight during June and July (Lawford and Cohen, 1989) and Inuvik's winter minimum is colder (Figure 5(a) and (b)).

Churchill is substantially wetter than Inuvik (Figure 5). At Churchill the annual precipitation (Figure 5(a)) varies from 272 mm (1964) to 618 mm (1983), and at Inuvik, from 110 mm (1995), to 350 mm (1962). The trend lines show a slight increase in precipitation for Churchill but a slight decrease for Inuvik over the 40-year record (Figure 5(a)). The maximum monthly precipitation occurs in August at both Churchill and Inuvik (Figure 5(b)).

3. THEORY AND METHODS

3.1. Surface energy budget

The surface energy balance is given by

$$Q^* = Q_G + Q_H + Q_E \quad [\mathrm{W\,m^{-2}}], \tag{1}$$

where Q^* is the net radiative flux at the surface, Q_G is the ground heat flux, Q_H is the sensible heat flux and Q_E is the latent heat flux.

Net radiation (Q^*) and incoming solar radiation ($K\downarrow$) were measured at all sites using REBS net radiometers and Epply pyranometers, respectively. Both instruments were sampled every ten seconds by Campbell 21X dataloggers and half-hourly averages were recorded.

Vegetated surfaces generally have a mean daily soil heat flux (Q_G) one or two orders of magnitude smaller than the major terms in the surface energy balance (Brutsaert, 1982). However, on shorter temporal scales, Q_G can be quite important. In permafrost environments, the ground heat flux can be substantial on longer time scales. Permafrost soils add complexity to the ground heat flux, during the melt and freeze back periods due to the large contribution of the latent heat of fusion. The subsurface soil temperatures, and Q_G, are a function of the solar radiation, soil texture, soil moisture content and state, in addition to the surface vegetation cover and weather conditions (Williams and Smith, 1989).

The net rate of heat flowing through the soil layer must equal the rate of change of internal energy in that volume. Thus, the ground heat flux (Q_G) can be quantified as

$$Q_G = C_S \frac{\partial T}{\partial t} \partial z \quad [\mathrm{W\,m^{-2}}], \tag{2}$$

where C_S (MJ $\mathrm{K^{-1}\,m^{-3}}$) is the depth-integrated volumetric heat capacity of the substrate, T (K) is the temperature of the substrate at depth z (m) and time t (s).

At Cw, the Bowen ratio energy balance (BREB) method was used to measure the surface energy budget and at Wd and Ww, the eddy correlation (EC) method was employed.

Q_H and Q_E can be related through the *Bowen ratio* (β)

$$\beta = \frac{Q_H}{Q_E}. \tag{3}$$

The sensible and latent heat fluxes can then be described using a time-averaged flux-gradient approach

$$Q_H = -\rho C_p K_H \frac{\Delta T_a}{\Delta z} \quad [\mathrm{W\,m^{-2}}], \tag{4}$$

$$Q_E = -\rho \frac{C_p}{\gamma} K_W \frac{\Delta e}{\Delta z} \quad [\mathrm{W\,m^{-2}}], \tag{5}$$

where ρ (kg $\mathrm{m^{-3}}$) is the density of air, C_p (MJ $\mathrm{kg^{-1}\,K^{-1}}$) is the specific heat of air, K_H and K_W ($\mathrm{m^2\,s^{-1}}$) are the turbulent transfer coefficients for sensible and latent heat, respectively, and γ (kPa $\mathrm{K^{-1}}$) is the psychrometric constant.

The eddy correlation method of measuring the surface energy fluxes is based on determining the turbulent fluxes of water vapour, momentum and sensible heat from the covariances of their respective eddies. This measures the turbulent exchange directly without restrictive assumptions as to the nature of the surface and the transfer mechanisms involved (Peixoto and Oort, 1992).

The mean vertical flux of the sensible and latent heat fluxes may be obtained via

$$Q_H = \rho C_p \overline{w'T'} \quad [\mathrm{W\ m^{-2}}], \tag{6}$$

$$Q_E = L\rho \overline{w'q'} \quad [\mathrm{W\ m^{-2}}], \tag{7}$$

where ρ (kg m^{-3}) is the density of air, C_p (MJ kg^{-1} K^{-1}) is the heat capacity of the air, L (MJ kg^{-1} kPa^{-1}) is the latent heat of vaporization, w' (m s^{-1}), T' (K) and q' (kPa) are the instantaneous variances in the vertical windspeed, air temperature and specific humidity all measured at the same height.

The covariance between w', q' and T' is made by electronic analog computation consisting of a multiplication and averaging process on Campbell Scientific 21X dataloggers. The Campbell processor calculates a simple statistical covariance for a given time period, and if there is more than one time period in the output interval it averages the covariance results (denoted by the overbar in Equations (6) and (7)). At Ww, the wind measurement is made using a Young propeller vertical anemometer, while at Wd, a three axis sonic anemometer is used. The temperature fluctuations at both TVC sites are measured using fine-wire copper–constantan thermocouples. In this study, only Q_H is measured directly, and the latent heat flux is solved as a residual in the energy balance equation

$$Q_E = Q^* - Q_H - Q_G \quad [\mathrm{W\ m^{-2}}]. \tag{8}$$

EC has three essential requirements to ensure valid measurements: (1) the response time of the sensor must be sufficiently fast to detect the smaller, higher frequency ($\sim$ 10 Hz) eddies; (2) the averaging period over which the covariances are calculated must be long enough to ensure that the larger, lower frequency eddies are detected; and (3) the orientation and placement of the windspeed sensors must be precise to ensure that the correlations involving one or more velocity components are accurate (Brutsaert, 1982). The propeller EC system underestimates Q_H due to the fact that if the response of the anemometer is slower than the higher frequency eddies so that part of the cross-correlation is undetected, and the flux is underestimated (Brutsaert, 1982). The vertical windspeed mean, which is separated from the short time fluctuations, is subject to larger time-scale trends. Therefore, the averaging period should be as short as possible to ensure that the time series remains stationary but long enough to cover even the slowest fluctuations of the turbulent spectrum (Brutsaert, 1982). The averaging periods in use at Ww and Wd are 10 min, with sensors sampling every 0.1 s. The vertical wind sensors must be at a height that satisfies fetch requirements and the sampling sensitivity of the instrument. At both Ww and Wd the sensors were placed at 3.2 m above the surface, adjacent to the temperature sensors. The vertical wind propeller anemometers were calibrated against a BREB system and a three-dimensional sonic anemometer. The propeller was found to underestimate the sonic and BREB system by 23%. The EC measurements were also corrected using the frequency response method utilized in previous studies (Moore, 1986; Blanford and Gay, 1992). Analysis of the net system cospectral transfer function, the dynamic frequency response of the wind and temperature sensors and the frequency cospectrum of the turbulence over a range of frequencies produced a similar result to the BREB/Sonic comparison. All the evidence indicates that the EC calculation of Q_H underestimates the actual flux by 23%, over the entire season. This value falls in the mid-range of observations made in previous studies which produced underestimations in the range of 4–48% (Tsvang *et al.*, 1973; Wesely and Hicks, 1975; Moore, 1986; Blanford and Gay, 1992). Thus, the Q_H measurements at Ww were corrected by a factor of 1.29 to account for this underestimation.

3.2. Error analysis

The numerous variables required to be measured and calculated in determining the energy budget inevitably leads to potential errors. For this study, previous error analysis results are used to estimate the errors characteristic of surface energy budget measurement.

Errors encountered while using the BREB method to determine the latent heat flux is a function of the errors inherent in the measurement of net radiation, ground heat flux and vertical air temperature and vapour pressure gradients. The estimated error in calculating the latent heat flux using the BREB approach is $\pm 23\%$ (Lafleur, 1988; Boudreau, 1993).

The EC systems employed at the Ww and Wd sites quantified the latent heat flux as a residual of the surface energy balance Equation (10). Thus, the error associated with this calculation is a function of the measurement of the net radiation, ground heat flux and sensible heat flux. The latent heat flux solved as a residual with the eddy correlation measurements is observed to have a RMSE of approximately $\pm 23\%$, which is very similar to that which has been reported for the BREB approach.

4. RESULTS

To facilitate comparisons, data are divided into three periods based on the phenology of the vascular plants. These periods are: (1) final snowmelt and pre-growth (1–21 June); (2) growth (22 June–8 August); (3) senescence (9–29 August). The first period (final snowmelt and pre-growth) encompasses the time over which the snow pack completely dissipates, and standing water is frequently observed at all sites. This period is characterized by temperatures in the range -10 to $+10$°C and continues until 'bud burst' occurs and greening of the canopy begins. The second period (growing) is characterized by a greening canopy and mean air temperatures in excess of 10°C.

Figure 6 compares the two study regions in terms of the energy available to drive the surface energy budget using potential insolation to establish that the radiation regime in these two different geographical locations is similar, and the regions can legitimately be compared. Region C, due to its lower latitude, experiences more potential insolation (I_0) during the spring and fall periods (Figure 6), whereas Region W has larger I_0 during the summer period. Overall, summer totals and patterns are very similar.

4.1. Growing season 1996

Averages for incident solar ($K\downarrow$) and net radiation (Q^*), expressed in proportion of potential insolation, measured at the three sites were quite similar (Figure 7) thus allowing for ready intercomparisons. Before

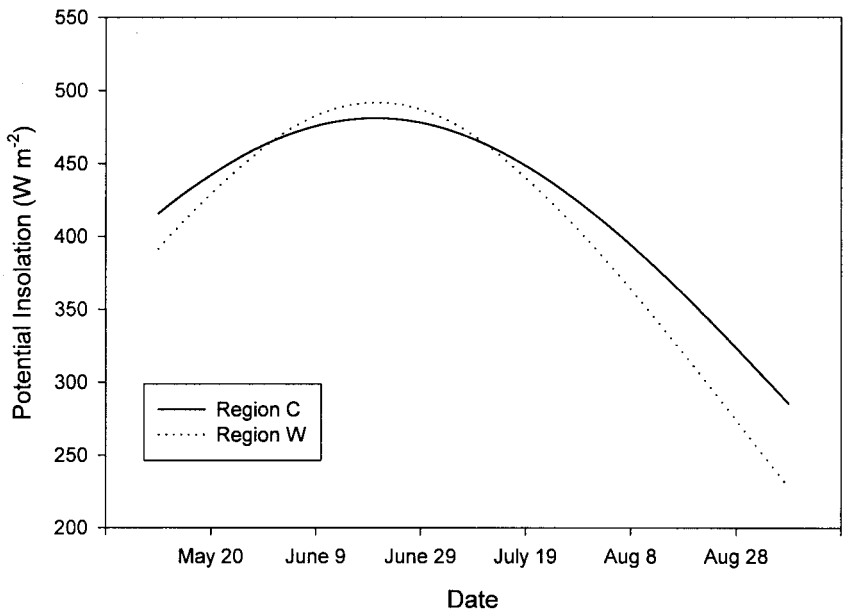

Figure 6. Seasonal variation in potential insolation for Region C and Region W

the summer solstice, Region W experienced larger $K\downarrow$ than did Region C. The solar radiation was maximum at the summer solstice with both locations receiving approximately 350 W m^{-2}. The seasonal means in $K\downarrow$ were 215 and 199 W m^{-2} for Region C and Region W, respectively. The smaller Q^* for Region W early in the season was a result of later-lying snow cover. Seasonal air temperatures were similar for all three sites (Figure 8). Cw had a mean of 11.1°C, and Ww and Wd had means of 9.5 and 10.1°C, respectively. It rained about twice as much at Region C (177 mm) than at Region W (80 mm).

Q^* at Cw (Table III) was approximately 20% larger than for Ww and Wd during the growth and senescence periods because of larger $K\downarrow$ (Figure 7). The seasonal net radiation was 25% larger at Cw (125 W m^{-2}) than at Ww and Wd (100 and 104 W m^{-2}, respectively).

The average Q_E for Cw, Ww and Wd was 71, 63 and 52 W m^{-2}, respectively, and the corresponding Q_H was 37, 32 and 31 W m^{-2}, respectively. Q_H thus accounted for more than 30% of Q^* at all sites, over the entire season (Table III). There was a clear decrease in Q^* and Q_E over the season for all sites (Table

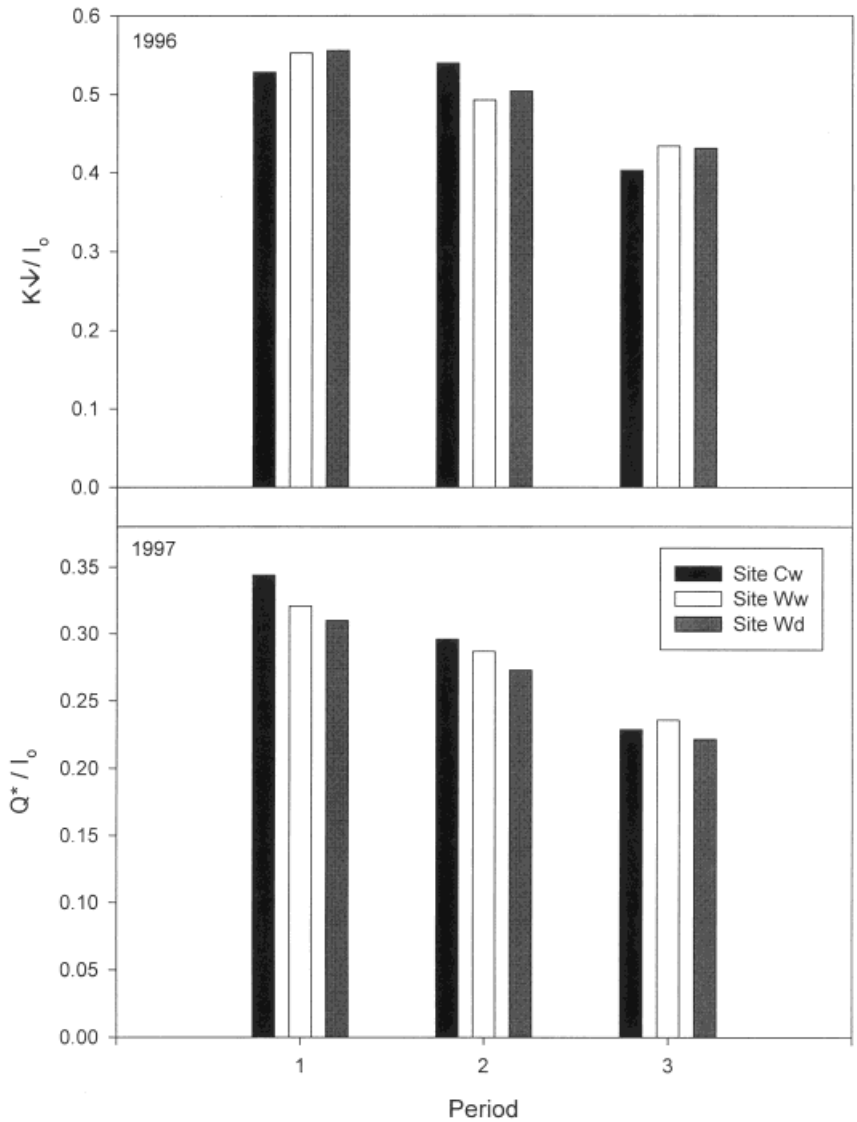

Figure 7. The ratios of incident solar radiation to potential insolation ($K\downarrow/I_0$) and of net radiation to potential insolation (Q^*/I_0) for 1996 and 1997

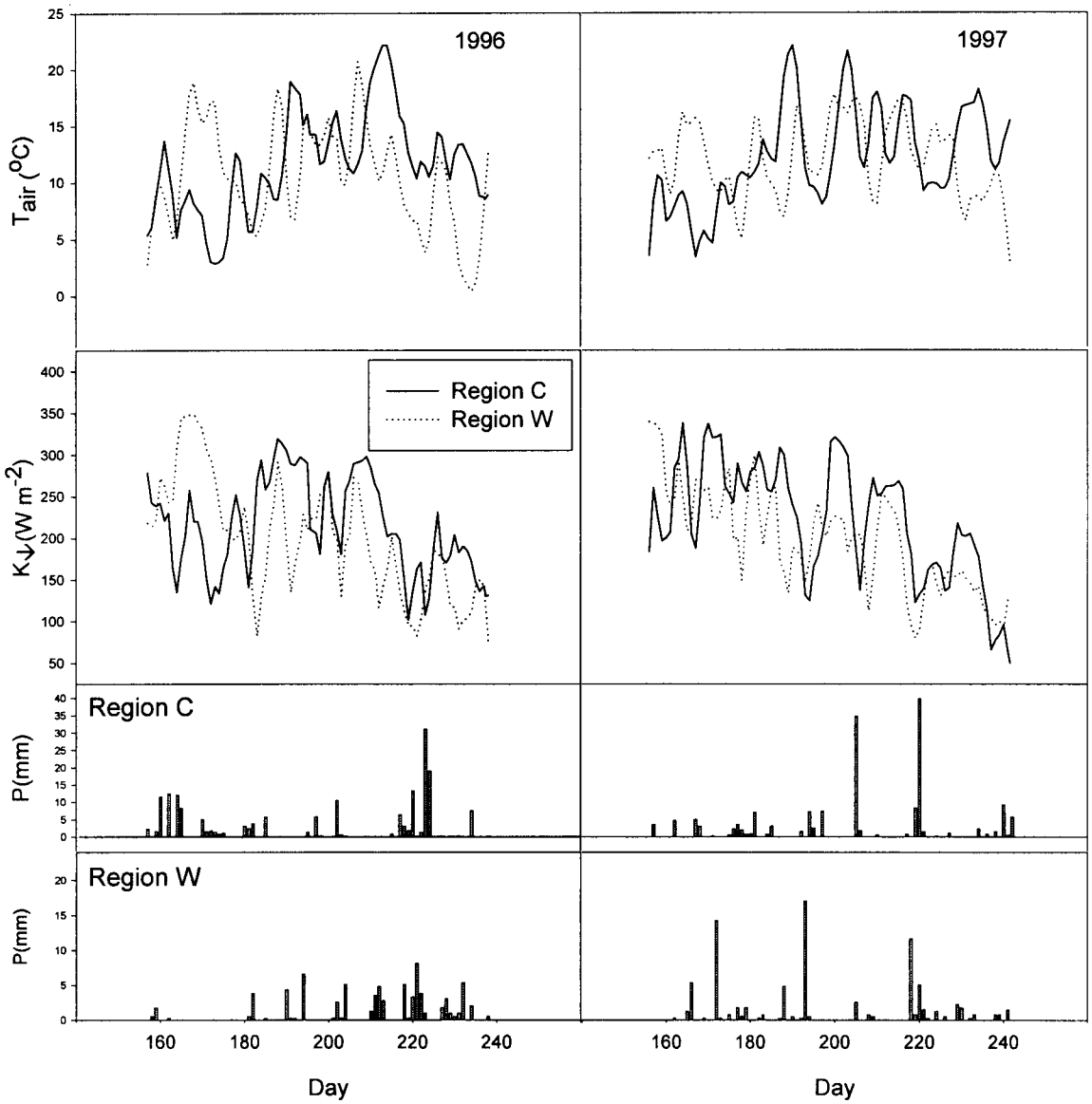

Figure 8. Air temperature (T), incident solar radiation ($K\downarrow$) and precipitation (P) for the two study regions in 1996 and 1997

III). However, the ratio Q_E/Q^* showed no seasonal trend (Table III) and all three sites exhibited maximum values of Q_E/Q^* in Period 3.

Immediately following snowmelt the appearance of bare ground led to a rapid change in the ground temperature profile and promoted a flux of heat into the frozen ground (Table III). This flux was larger at the Wd site (21 W m^{-2}) than Ww (5 W m^{-2}) and Cw (17 W m^{-2}). Ww with the smallest ground heat fluxes, had the shallowest active layer throughout the season (Figure 4). The small thermal diffusivity of its thick sphagnum mat suppressed the development of large ground temperature gradients. In contrast, Wd produced the deepest active layer ($\sim$0.80 m) due to the large Q_G favoured by the mixed soils and sparser surface vegetation cover.

During the full season, Cw had the highest evaporation rate at 2.6 mm day^{-1}, followed by Ww and Wd with rates of 2.3 and 1.8 mm day^{-1}, respectively. The two wetland sites had very similar magnitudes and trends, despite their very different geographical locations, physical characteristics and rainfall amounts

(Figure 9). The cumulative water deficit decreased at the same relative rate for both of the Region W sites, demonstrating substantially more water withdrawal from these two sites than from Cw. Cw's water deficit decreased substantially during the very wet period around the transition from Period 2 to 3 and Ww experienced a greater water deficit by the end of the season.

4.2. Growing season 1997

The early season trend in air temperature was similar to that observed in 1996 (Figure 8). The seasonal trend in $K\downarrow$ showed that Region W experienced more cloudy periods early in the season, whereas Region C experienced an increase in clouds later in the season. Overall, 1997 was a warmer season for Region W, than was 1996. For 1997, the air temperature at Ww, Wd and Cw were virtually identical.

The total seasonal precipitation amounts were similar to 1996. The magnitude of extreme events increased but their frequency decreased for all locations (Figure 8). As in 1996, Region C received twice

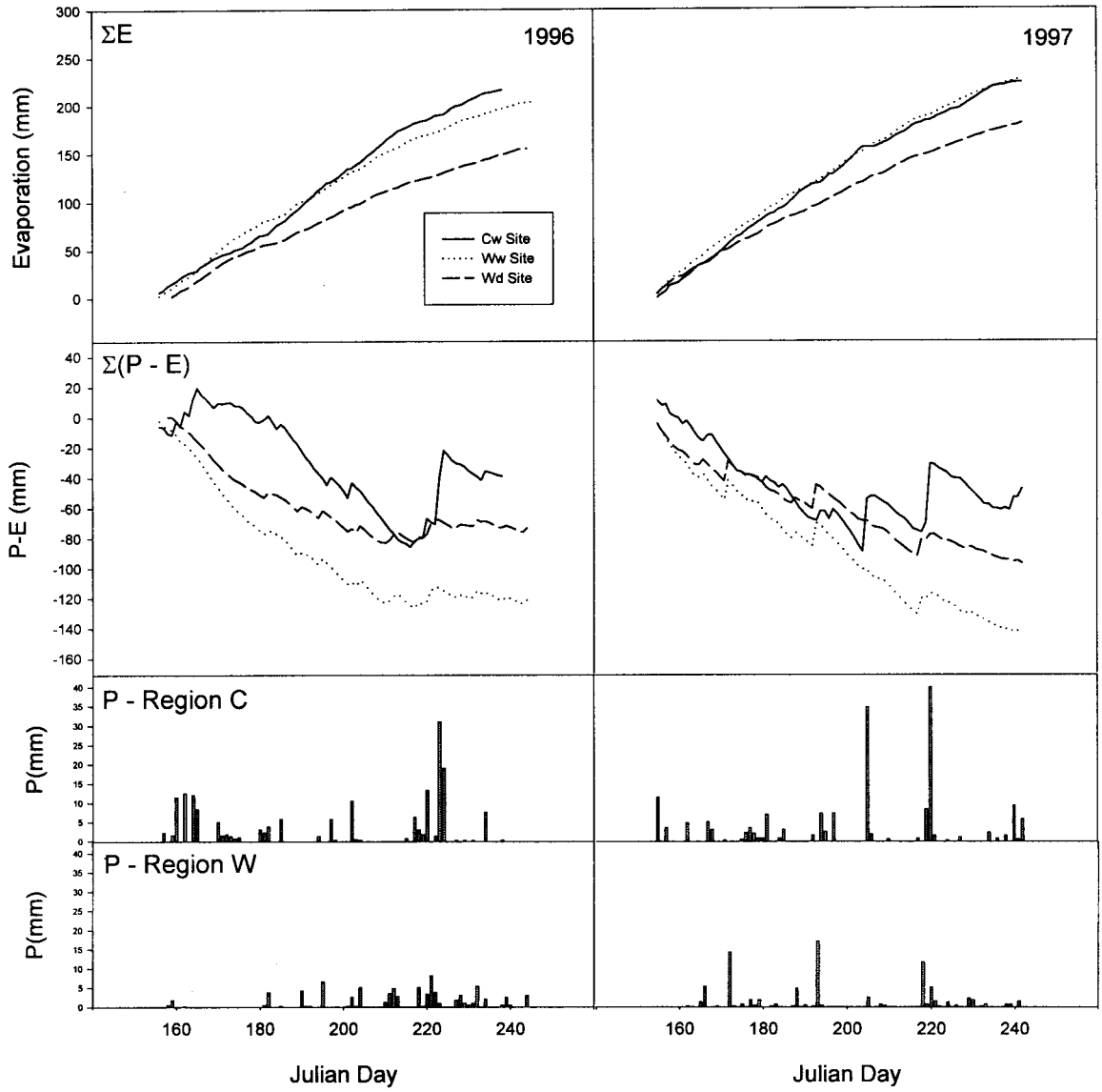

Figure 9. Cumulative evaporation (ΣE), water deficit ($\Sigma(P-E)$) and precipitation (P) for the three sites in 1996 and 1997

as much precipitation (176 mm) as Region W (84 mm). The mean precipitation amounts at the two locations were 5.2 mm at C and 2.4 mm at W which is very similar to the 1996 values.

Similar to 1996, Q^* decreased steadily over the course of the season for all sites (Table III). Seasonal Q^* at Cw was 10 and 15% larger than the average for Ww and Wd, respectively, less than the 25% difference observed in 1996 (Table III). As in 1996, Ww had the highest Q_E in the pre-growth period. However, in contrast to 1996, Q_E at Ww was highest of all sites during the growth period. During the senescence period, Cw and Ww had virtually identical Q_E. Seasonally, sites Cw and Ww had the largest Q_E values. Q_E exhibited a very similar seasonal trend to that observed in 1996. (Table III). However, Cw reaches its lowest Q_E in the first period, and the two W sites experience their respective minima in Q_E during Period 2 as a result of the increased incidence of large rain events during that period.

Q_H was much smaller for Ww and Wd than for Cw in the pre-growth period, and smaller for Cw during the senescence period (Table III). Seasonal Q_H for 1997, was largest for Cw and Ww. Q_H accounted for at least 30% of Q^* for all sites (Table III). The Bowen ratio behaved similarly to 1996 (Table III).

Ww and Cw had the lowest seasonal Q_G (averaging 6 and 17 W m^{-2}, respectively) and Wd again showed the largest (23 W m^{-2}) (Table III).

Cw and Ww evaporated at approximately the same rate as during 1996 (2.5 and 2.6 mm day^{-1}, respectively) (Figure 9). However, the evaporation rate (2.1 mm day^{-1}) for Wd increased substantially compared with its 1996 values. The cumulative water deficits for all of the sites increased at the same relative rate.

4.3. Surface response to temperature forcing

Due to the regular interplay between cold and warm air masses in summer at these subarctic sites there were frequent and large changes in temperature and vapour deficit. The impact of these changes on the surface energy balance was ascertained by examining the coldest and warmest days as defined by lower and upper quartiles of mean daily temperatures.

Averaged for both years, the upper quartile temperatures were 12.1, 12.3 and 11.5°C warmer than the lower quartile ones at Cw, Ww and Wd, respectively (Table II). At Cw and Ww the differences were largest in Period 2 and least in Period 3 (Table III). However, at Wd the difference was largest in Period 1. Rainfall was greater during cold than warm periods at all sites (Table II). Rainfall amounts were small during Period 1 at all sites and differences during warm and cold periods were insignificant (Table III). In Period 2 all sites received most of their seasonal rainfall during cold conditions, with Cw showing the largest difference between the warm and cold quartiles. In Period 3 only Cw demonstrated a significant difference between the two quartiles.

All fluxes showed large differences in absolute magnitude under hot, clear conditions (Table II). Under warmer conditions Q^* was significantly larger than under cooler conditions at all sites. Similarly, under hot conditions, Q_E exceeded the cold condition amount by $\sim 100\%$. Similar differences in magnitude were

Table II. Mean values of air temperature (T), precipitation (P), net radiation (Q^*), latent heat flux, sensible heat flux and ground heat flux (Q_E, Q_H, Q_G), during hot and cold conditions at the three sites averaged for the 2 years of measurement

	Cw Hot	Cw Cold	Ww Hot	Ww Cold	Wd Hot	Wd Cold
T (°C)	17.9	5.8	17.5	5.2	17.2	5.7
P (mm)	8.4	46.8	1.9	3.0	1.9	3.1
Q^* (W m^{-2})	141.9	84.7	132.0	90.1	128.5	90.2
Q_E (W m^{-2})	92.2	44.0	91.1	56.8	69.4	48.7
Q_H (W m^{-2})	24.1	33.0	29.0	29.7	29.6	29.8
Q_G (W m^{-2})	24.1	8.5	11.9	2.7	33.4	12.6

'Hot' is the upper temperature quartile and 'Cold' is the lower temperature quartile.

Table III. Mean values for air temperature (T), precipitation (P), net radiation (Q^*), the ratios of latent heat flux, sensible heat flux and ground heat flux to net radiation (Q_E/Q^*, Q_H/Q^*, Q_G/Q^*) and Bowen ratio (β), during hot and cold conditions at the three sites averaged for the 2 years of measurement

		Cw Hot	Cw Cold	Ww Hot	Ww Cold	Wd Hot	Wd Cold
T	S	17.9	5.8	17.5	5.2	17.2	5.7
	1	14.6	2.8	18.6	4.7	19.0	5.8
	2	21.8	5.6	19.6	5.7	18.8	6.0
	3	17.5	8.9	14.2	5.1	13.8	5.3
Rain	S	8.4	46.8	1.9	3.0	1.9	3.1
(mm)	1	6.3	7.5	0.0	0.2	0.0	0.3
	2	0.7	28.9	0.3	7.2	0.3	7.2
	3	1.4	10.4	1.6	1.7	1.6	1.7
Q^*	S	141.9	84.7	132.0	90.1	128.5	90.2
(W m^{-2})	1	185.9	101.5	174.3	135	179.2	130.5
	2	138.1	86.8	138.5	70.9	128.7	79.5
	3	101.7	65.9	83.3	64.4	77.6	60.7
Q_E/Q^*	S	0.65	0.52	0.69	0.63	0.54	0.54
	1	0.62	0.47	0.70	0.56	0.54	0.43
	2	0.67	0.53	0.68	0.63	0.53	0.51
	3	0.67	0.55	0.70	0.70	0.55	0.67
Q_H/Q^*	S	0.17	0.39	0.22	0.33	0.23	0.33
	1	0.22	0.43	0.23	0.40	0.23	0.37
	2	0.15	0.44	0.24	0.31	0.25	0.33
	3	0.14	0.31	0.19	0.28	0.20	0.29
Q_G/Q^*	S	0.17	0.10	0.09	0.03	0.26	0.14
	1	0.16	0.09	0.13	0.04	0.26	0.22
	2	0.17	0.10	0.06	0.06	0.24	0.17
	3	0 18	0.12	0.07	0.00	0.28	0.04
Bowen ratio	S	0.30	0.82	0.32	0.53	0.42	0.65
	1	0.40	0.95	0.35	0.75	0.45	0.85
	2	0.30	0.85	0.35	0.45	0.45	0.65
	3	0.20	0.65	0.25	0.40	0.35	0.45

S is the seasonal average, 'Hot' is the upper temperature quartile and 'Cold' is the lower temperature quartile.

also seen for Q_H and Q_G (Table II). Q_H was less in absolute magnitude and Q_G was approximately three times larger under warmer conditions.

Seasonally, Cw and Ww had larger Q_E/Q^* during warm conditions. Cw demonstrated the largest difference in Q_E/Q^* between quartiles (Table III). All three sites showed their largest increase in Q_E/Q^* under warmer conditions during Period 1, and the smallest during Period 3. Wd actually showed a decrease in Q_E/Q^* for the upper quartile in Period 3.

On a seasonal basis the cold condition Q_H/Q^* values were larger than the warm ones, with Cw showing the largest difference (0.22) (Table III). At Cw the difference was largest in Period 2, but at Ww and Wd they are largest in Period 1. Seasonally, Q_G/Q^* was greater during warm conditions for all sites, with Wd showing the largest difference.

Seasonally, the Bowen ratio was larger during cold conditions for all sites, with Cw showing the largest increase (0.52) and Ww showing the smallest increase (0.21) (Table III). All sites demonstrated a decrease in the Bowen ratio over the course of the season for both quartiles.

5. DISCUSSION

The total precipitation measured at Region C over the two study seasons was approximately two times greater than that measured at Region W (Table IV). Although the precipitation was two times greater, Q_E/Q^* was the same. Thus, wetlands apparently evaporate at equal rates and water at both sites was non-limiting.

The air temperatures and extraterrestrial solar radiation observed at the three locations over the two study seasons were within 10% of each other (Table IV). Therefore, temperature forcing and radiation forcing on the surface energy balance was very similar. The air temperature at Cw was slightly warmer than the historical seasonal value of 9.8°C, and the Ww and Wd temperatures were slightly cooler than the historical value of 11.8°C.

The average Q^* over the two seasons for Ww was only 1% larger than that for Wd, which was not greater than expected errors in the radiometers used in the study. However, Q^* at Cw was 20% higher than at the two W sites (Table IV). This was due to larger net solar radiation (K^*) a consequence of greater $K\downarrow$ and a smaller albedo.

The ground heat flux showed substantial variability between the different sites, and to a lesser extent, between periods. Wd had the largest ground heat flux because it had the highest mineral soil content and shallowest organic layer. These factors led to a high soil thermal diffusivity which promoted a large active layer depth over the course of the season (Monteith and Unsworth, 1990). Conversely, Ww had the lowest Q_G at all times. The extensive sphagnum mat found at this site insulated the thick organic layer, thereby suppressing the ground heat flux.

Sensible heat fluxes were very similar for all locations, all seasons and both years. Most importantly, the two wetland sites had fairly constant and similar evaporation regimes. The Q_E for Cw and Ww were within 7% of each other (Table IV). The Q_E for both wet sites were approximately 20% greater than Wd, which while substantially and consistently less than the two wet sites, should be interpreted with some caution in light of the potential error in the measurements. The extensive sphagnum moss cover at Ww was effective at storing surface water, contributing to both surface evaporation and transpiration. Thus, the wetland sites appeared to be non-limited in water supply.

The cumulative evaporation amounts for the two wetland sites were within 5% of each other in both years, and the upland dry site was consistently 15–25% less than the wetland sites. The close similarity of the evaporation rates from the two wetland sites suggests that their peat substrate was very important in governing the evaporation regime. While both sites were wetlands, there were significant differences in surface cover, water table and microtopography. Most importantly, there was generally no standing water at Ww as opposed to Cw. Thus, the hydraulic properties of the peat present at both sites, was important in providing an available source of moisture for evaporation. The magnitude of the latent heat flux from

Table IV. Total values of precipitation, temperature, evaporation and mean values of energy balance terms for both years of measurement

	Cw	Ww	Wd
Precipitation (mm)	353	166	166
T (°C)	11.9	10.7	11.1
I_0 (W m^{-2})	425	411	411
$K\downarrow$ (W m^{-2})	231	200	201
Albedo	0.12	0.20	0.18
Q^* (W m^{-2})	129	107	106
Q_E/Q	0.57	0.64	0.52
Q_H/Q^*	0.29	0.29	0.28
Q_G/Q	0.14	0.06	0.22
Bowen ratio	0.51	0.45	0.54
Evaporation (mm)	439	432	336

Symbols are defined in Figures 7 and 9 and in Table II.

these wetland sites indicated that they were very efficient evaporators. The abundance of wetlands, in these regions suggests that during the summer snow-free period, they can provide a significant source of moisture to enhance regional precipitation.

Q_H/Q^* was small for the warm temperatures at all sites, during all periods (Table III). The largest Q_E/Q^* for all sites was correlated with warm temperatures. The strong dependence of the latent heat flux on temperature illustrates that the available energy and moisture may not be the only important forcing mechanisms. Other factors associated with the temperature changes, involve mesoscale or synoptic scale influences (Rouse *et al.*, 1987, 1992; Rouse, 1991). In general, the western sites (Ww and Wd) are less sensitive to the warm/cold temperature changes. This suggests that mesoscale effects may be less important at these sites due to them being further from the Arctic Ocean than the central site.

The relationship between the surface energy balance and synoptic conditions is important. The link between the surface and synoptic climatologies will provide insight into the impacts of changing weather systems on the surface energy and water cycles on a regional scale.

6. CONCLUSIONS

The western and central subarctic wetland sites are both evaporated at similar rates during the period of study. Because the central site has twice the precipitation and has standing water for part of the growing season, but has a very similar evaporation rate to the Ww site, it is concluded that there are restrictive controls on the evaporation rates, exerted through the radiation regime, the ground heat flux and atmospheric temperature and vapour pressure.

Although net radiation at Site Cw is 21% larger than at Site Ww the ground heat flux is less than one-half as great. The latter is manifest in shallow active layer depths at Ww. Major surface restriction on the ground heat flux at site Ww is exerted by microtopography and the large thermal insulating properties of sphagnum moss. The result is that the available energy at the surface ($Q^* - Q_G$) at Ww comes close in magnitude to that at Cw. The well-drained subarctic dryland has a distinctive surface energy balances compared to its wetland counterparts. Evaporation rates are about three-quarters and they are not significantly influenced by temperature.

Temperature strongly influences the other surface energy fluxes at all sites. Temperature and vapour pressure deficit are autocorrelated with cold temperatures associated with small vapour pressure deficit and warm ones with large vapour pressure deficit. Cold temperatures stifle evaporation rates and warm temperatures enhance them at both wetland sites. During cold temperatures Q_H is enhanced and Q_G is stifled in comparison to warm conditions. The strong radiation and temperature–vapour pressure controls indicate that synoptic systems are very important to evaporation rates and magnitudes, and to the other surface energy fluxes, which is the focus of the second paper in this set.

In summary, the two wetland sites demonstrated similar evaporation behaviours, but the dryland site evaporates much less. This similarity in wetland evaporation and dissimilarity between wet and dryland evaporation demonstrates the importance of the surface organic layer in transporting and storing water for evaporation. Also, the magnitude of the convective and conductive heat fluxes is shown to be strongly correlated with temperature in both regions, with warm temperatures enhancing the latent and ground heat fluxes while suppressing the sensible heat flux at all sites. This temperature effect on the surface regime emphasizes the need to examine the interactions between the synoptic climatology of a region and the surface energy and water budgets.

Therefore, surface vegetative characteristics and microtopography influence the surface moisture conditions, which can interact with the atmospheric controls.

ACKNOWLEDGEMENTS

Financial support for this research has been provided by the Natural Science and Engineering Council of Canada and by student northern training grants from the Canada Department of Indian and Northern

Affairs. The authors would like to thank the Churchill Northern Studies Centre, Aurora College and especially the Polar Continental Shelf Project for field and logistical support. Finally, the authors gratefully acknowledge improvements and corrections suggested by the reviewers.

REFERENCES

Blanford JH, Gay LW. 1992. Tests of a robust eddy correlation system for sensible heat flux. *Theoretical and Applied Climatology* **46**: 53–60.

Boudreau LD. 1993. The energy and water balance of a high subarctic wetland underlain by permafrost, Unpublished MSc Thesis. McMaster University, Canada, 205 pp.

Boudreau LD, Rouse WR. 1995. The role of individual terrain units in the water balance of wetland tundra. *Climate Research* **5**: 31–47.

Brutsaert W. 1982. *Evaporation into the Atmosphere*. D. Reidel Publishing Co: Holland; 299 pp.

Ecoregions Working Group and Canada Committee on Ecological Land Classification. 1989. *Ecoclimatic Regions of Canada: First Approximation*, *Ecological Land Classification Series No. 23*. Canadian Wildlife Service, Conservation and Protection, Environment Canada: Ottawa; 119 pp.

Guo Y, Schuepp PH. 1994. On surface energy balance over the northern wetlands 1. The effects of small-scale temperature and wetness heterogeneity. *Journal of Geophysical Research* **99**(D1): 1601–1612.

Intergovernmental Panel on Climate Change. 1992. *Climate Change 1995. Impacts, Adaptations and Mitigation of Climate Change. Scientific-Technical Analyses*. Cambridge University Press: Cambridge; 879 pp.

Lafleur PM. 1988. Surface cover and air mass controls on evaporation from a subarctic marsh, Unpublished PhD Thesis. McMaster University, Canada, 165 pp.

Lawford RG, Cohen SJ. 1989. The impacts of climatic variability and change in the Mackenzie Delta. In *Mackenzie Delta Environmental Interactions and Implications of Development*, *Proceedings of the Workshop on the Mackenzie Delta, 17–18* October *1989*, Marsh P, Ommaney CSL (eds). NHRI: Saskatoon, Saskatchewan.

Marsh P, Pomeroy JW. 1996. Meltwater fluxes at an arctic forest–tundra site. *Hydrological Processes* **10**: 1383–1400.

Maxwell B. 1997. Responding to Global Climate Change in Canada's Arctic. Volume 2 of The Canada Country Study. Climate Impacts and Adaptation, Environmental Adaptation Research Group, Atmospheric Environment Service, Environment Canada. Downsview, Ontario, 82 pp.

Monteith JL, Unsworth MH. 1990. *Principles of Environmental Physics* (2nd edn). Routledge, Chapman and Hall: New York; 241 pp.

Moore CJ. 1986. Frequency response corrections for eddy correlation systems. *Boundary-Layer Meteorology* **37**: 17–35.

National Wetlands Working Group. 1987. *The Canadian Wetland Classification System*, *National Wetlands Working Group of the Canada Committee on Ecological Land Classification. Ecological Land Classification Series*, *No. 21*. Land Conservation Branch, Canadian Wildlife Service, Environment Canada: Ottawa, Ontario; 18 pp.

Peixoto JP, Oort AH. 1992. *Physics of Climate*. AIP Press: New York; 520 pp.

Petrone RM, Rouse WR. 2000. Synoptic controls on the surface energy and water budgets in subarctic regions of Canada. *International Journal of Climatology* **20**: 1149–1165.

Quinton WL. 1997. Runoff from hummock-covered arctic tundra hillslopes in the continuous permoirost zone, Unpublished PhD Thesis. University of Saskatchewan, Saskatoon, Canada, 277 pp.

Rouse WR. 1990. The regional energy balance. In *Northern Hydrology: Canadian Perspectives*, Prowse TD, Ommaney CSL (eds). NHRI Science Report No. 1: Saskatoon; 187–206.

Rouse WR. 1991. Impacts of Hudson Bay on the terrestrial climate of the Hudson Bay lowlands. *Arctic and Alpine Research* **11**: 24–30.

Rouse WR. 1998. A water balance model for a subarctic sedge fen and its application to climatic change. *Climatic Change* **38**: 207–234.

Rouse WR, Hardill SG, Lafleur PM. 1987. The energy balance in the coastal environment of James Bay and Hudson Bay during the growing season. *Journal of Climatology* **7**: 165–179.

Rouse WR, Carlson CW, Weick EJ. 1992. Impacts of summer warming on the energy and water balance of wetland tundra. *Climatic Change* **22**: 305–326.

Tsvang I R, Koprov BM, Zubkovskii SL, Dyer AJ, Hicks B, Miyake M, Stewart RW, McDonald JW. 1973. A comparison of turbulence measurements by different instruments: Tsimlyansk field experiment 1970. *Boundary-Layer Meteorology* **3**: 499–521.

Wesely ML, Hicks BB. 1975. Comments on 'Limitations of an eddy-correlation technique for the determination of the carbon-dioxide and sensible heat fluxes'. *Boundary-Layer Meteorology* **9**: 363–367.

Wessel DA. 1992. Modelling evaporation from a subarctic sedge wetland, Unpublished MSc Thesis. McMaster University, Hamilton, Canada, 169 pp.

Williams PJ, Smith MW. 1989. *The Frozen Earth Fundamentals of Geocryology*. Cambridge University Press: Cambridge; 302 pp.

Woo M-K, Lewkowicz AG, Rouse WR. 1992. Response of the Canadian permafrost environment to climatic change. *Physical Geography* **13**: 287–317.

